Short communication

# *In vivo* imaging of epileptic activity using 2-NBDG, a fluorescent deoxyglucose analog

Vassiliy Tsytsarev [a,b,1,2], Konstantin I. Maslov [a,1,3], Junjie Yao [a,1,3], Archana R. Parameswar [c,4], Alexei V. Demchenko [c,*], Lihong V. Wang [a,**]

[a] Department of Biomedical Engineering, Washington University in St. Louis, One Brookings Drive, St. Louis, MO 63130, USA
[b] Krasnow Institute for Advanced Study, Molecular Neuroscience Department, George Mason University, 4400 University Drive, Mail Stop 2A1, Fairfax, VA 22030, USA
[c] Department of Chemistry and Biochemistry, University of Missouri – Saint-Louis, One University Blvd., St. Louis, MO 63121, USA

## ABSTRACT

Accurately locating epileptic foci has great importance in advancing the treatment of epilepsy. In this study, epileptic seizures were first induced by intracortical injection of 4-aminopyridine in rats. A fluorescent deoxyglucose substitute, 2-(*N*-(7-nitrobenz-2-oxa-1,3-diazol-4-yl)amino)-2-deoxyglucose (2-NBDG), was then continuously injected via the tail vein. Brain glucose metabolism was subsequently monitored by fluorescence imaging of 2-NBDG. The initial uptake rate of 2-NBDG at the injection site of 4-aminopyridine significantly exceeded that of the control injection site, which indicated local hypermetabolism induced by seizures. Our results show that 2-NBDG can be used for localizing epileptic foci.

© 2011 Elsevier B.V. All rights reserved.

## 1. Introduction

In neurophysiology, localizing neuronal activity, especially epileptic seizures, is of great importance (Bahar et al., 2006; Bhatia et al., 2008; Cang et al., 2005; Fisher et al., 2004; Hielscher et al., 2002; Inyushin et al., 2010). In clinical practice, functional magnetic resonance imaging (fMRI) (Salek-Haddadi et al., 2003), positron emission tomography (PET) (Dedeurwaerdere et al., 2005; Sheth et al., 2009), optical coherence tomography (Srinivasan et al., 2010), and near-infrared spectroscopy (Hielscher et al., 2002; Lee et al., 2010) have all been used to locate epileptic foci. In preclinical studies, intrinsic optical signal imaging (IOS) (Inyushin et al., 2001; Ma et al., 2009; Tsytsarev et al., 2008) and voltage-sensitive dye optical imaging (VSD) have also been demonstrated for this purpose (Fisher et al., 2004, 2008; Kameyama et al., 2008; Takagaki et al., 2011; Tsytsarev et al., 2006, 2010).

In mammals, glucose is the primary energy source. Complete oxidation of glucose produces $CO_2$, water, and adenosine triphosphate (ATP). ATP can be used by any type of cells, including neurons and astrocytes (Nitin et al., 2009; Rouach et al., 2008). Perfusion-based brain imaging, which relies on the coupling between neuronal activity and glucose metabolism (Millon et al., 2011; Itoh et al., 2006, 2004; Inyushin et al., 2010), has become a popular method to localize epileptic foci by using derivatives of 2-deoxyglucose (2-DG). Among these, fluorodeoxyglucose ($^{18}$F) (FDG), a glucose analog with the radioactive isotope fluorine-18 substituted for the normal hydroxyl in the glucose molecule, is widely used in PET studies (Imamura et al., 2009; Katsuyama et al., 2010). Once injected into the body, FDG can be taken up by cells, where phosphorylation prevents it from being released again from the cells. However, because of the lack of the 2′-hydroxyl group needed for glycolysis, FDG cannot be further metabolized (Millon et al., 2011; Sheth et al., 2009). Therefore, the distribution of the trapped FDG is a good reflection of glucose metabolism. However, the ionizing radiation of FDG limits its repetitive usage.

Fluorescent 2-DG derivatives can act like FDG without the radiation concern (Yamada et al., 2009). In our study, we employed a fluorescent 2-DG analog, 2-(*N*-(7-nitrobenz-2-oxa-1,3-diazol-4-yl)amino)-2-deoxyglucose (2-NBDG), for visualization of *in vivo* epileptic activities induced by intracortical injection of 4-aminopyridine (4-AP). The increased uptake rate of 2-NBDG at the injection site of 4-AP reflected elevated cell metabolism caused by epileptic seizures. The results demonstrate that 2-NBDG has the
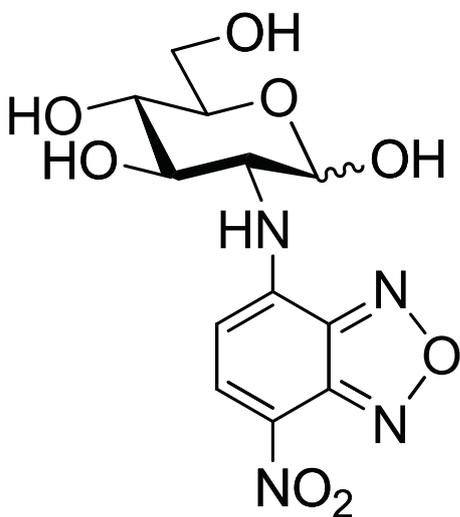
**Fig. 1.** 2-[*N*-(7-nitrobenz-2-oxa-1,3-diazol-4-yl)amino]-2-deoxy-D-glucopyranose (2-NBDG).

potential to be used as a contrast agent to image epileptic seizures *in vivo*.

## 2. Materials and methods

### 2.1. 2-NBDG synthesis

The synthesis of 2-NBDG (Fig. 1) was carried out using a modified procedure originally developed by Yamada et al. (2009). D-Glucosamine hydrochloride (1 g, 4.63 mM) was dissolved in methanol (10 mL), and NaHCO$_3$ (0.97 g) was added. The resulting mixture was stirred for 15–20 min. Then 1.11 g of 4-chloro-7-nitrobenzofuran (NBDCl) (5.56 mM) was added, and the reaction mixture was first stirred for 5 min at room temperature and then for an additional 45 min at 50 °C. After that, the solids were filtered out and the filtrate was concentrated *in vacuo*. The residue was purified by column chromatography, first on silica gel (methanol/dichloromethane gradient elution) and then on Sephadex LH-20 (methanol/dichloromethane, 1/1 (v/v) isocratic elution) (Bem et al., 2007). Pure fractions were combined and concentrated, and the residue was lyophilized from water to give 2-NBDG (200 mg, 13% yield) as an orange-red amorphous solid. The analytical data were essentially the same as reported previously by Yamada et al. (2009).

### 2.2. Fluorescence imaging system setup

The fluorescence imaging system is shown in Fig. 2. The light source was a 120-W xenon arc lamp with two excitation filters (450 ± 40 nm). Fluorescent images were captured by a low noise CCD camera. A 4× objective (NA: 0.1) with an emission filter (550 ± 40 nm) and an achromatic doublet (focal length: 100 mm) comprised the camera lens. The CCD camera was positioned above the brain chamber, with its optical axis adjusted to be as closely perpendicular to the cortical surface as possible. The focal plane was 500 µm below the surface of the dura mater (Bahar et al., 2006; Yang et al., 2002).

### 2.3. Animal preparations

For each experiment, a Sprague–Dawley adult rat (male, 250–350 g, 2–3 months) was anesthetized by an IP injection of a mixture of ketamine (90 mg/kg) and xylazine (12 mg/kg) and fixed onto an animal holder (Hu et al., 2009; Tsytsarev et al., 2011). Throughout the experiment, the animal was supplied with breathing grade compressed air (AI B300, Airgas, MO) and maintained under anesthesia using isoflurane (1.0–1.5% with an airflow rate of ~1 L/min). The body temperature of the animal was maintained at 37 °C by a temperature-controlled electrical heating pad. The hair on the scalp was removed using an electric shaver, and the scalp was incised along the midline. At the dorsal part of the skull, a cranial window of ~6–8 mm$^2$ was opened using a dental drill (Fig. 2, inset) (Tsytsarev et al., 2008).

A chamber made of silicone was placed above the cranial window. To suppress cortical tissue motion induced by respiratory and cardiovascular movements, the chamber was filled with high density silicone oil and then sealed with a cover glass. For the later continuous injection of 2-NBDG, a lateral tail vein was punctured with a sterile catheter after the tail was heated by warm water (35–40 °C). A cannula was inserted into the tail vein and fixed onto the tail with adhesive tape. At the end of each experiment, the animal was sacrificed by an overdose of Nembutal (200 mg/kg). All procedures were carried out according to the standards of the Animal Studies Committee of Washington University in St. Louis.

### 2.4. Inducement of epileptic seizures

After craniotomy, two intracortical injections were made. The first was 0.5 µL of 25 mM solution of 4-AP in artificial cerebrospinal fluid (ACSF), which was used to induce local epileptic seizures (Bahar et al., 2006; Yang et al., 2002). The second, as a control, was the same volume of ACSF, located 2–3 mm from the injection site of 4-AP. Both injections were done by an injector device (Nanojet II) with a 15-25 µm diameter glass microcapillary. The injector was mounted on a micromanipulator that allowed precise injections 0.5 mm below the surface (Dedeurwaerdere et al., 2005; Fisher et al., 2008).

### 2.5. Fluorescence imaging of 2-NBDG

Following the injections of 4-AP and ACSF, fluorescent images of the cerebral cortex were captured every 20 s, with an exposure time
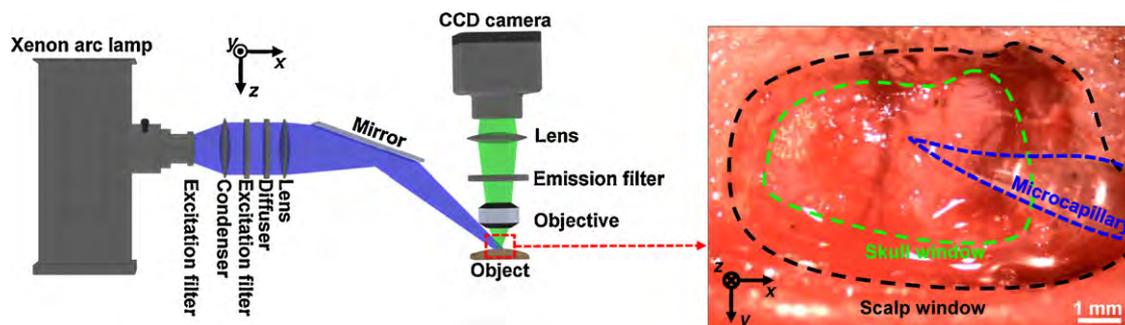


**Fig. 2.** Experimental setup. Inset: cranial opening with microcapillary for intracortical injection. x, rostral; y, lateral.
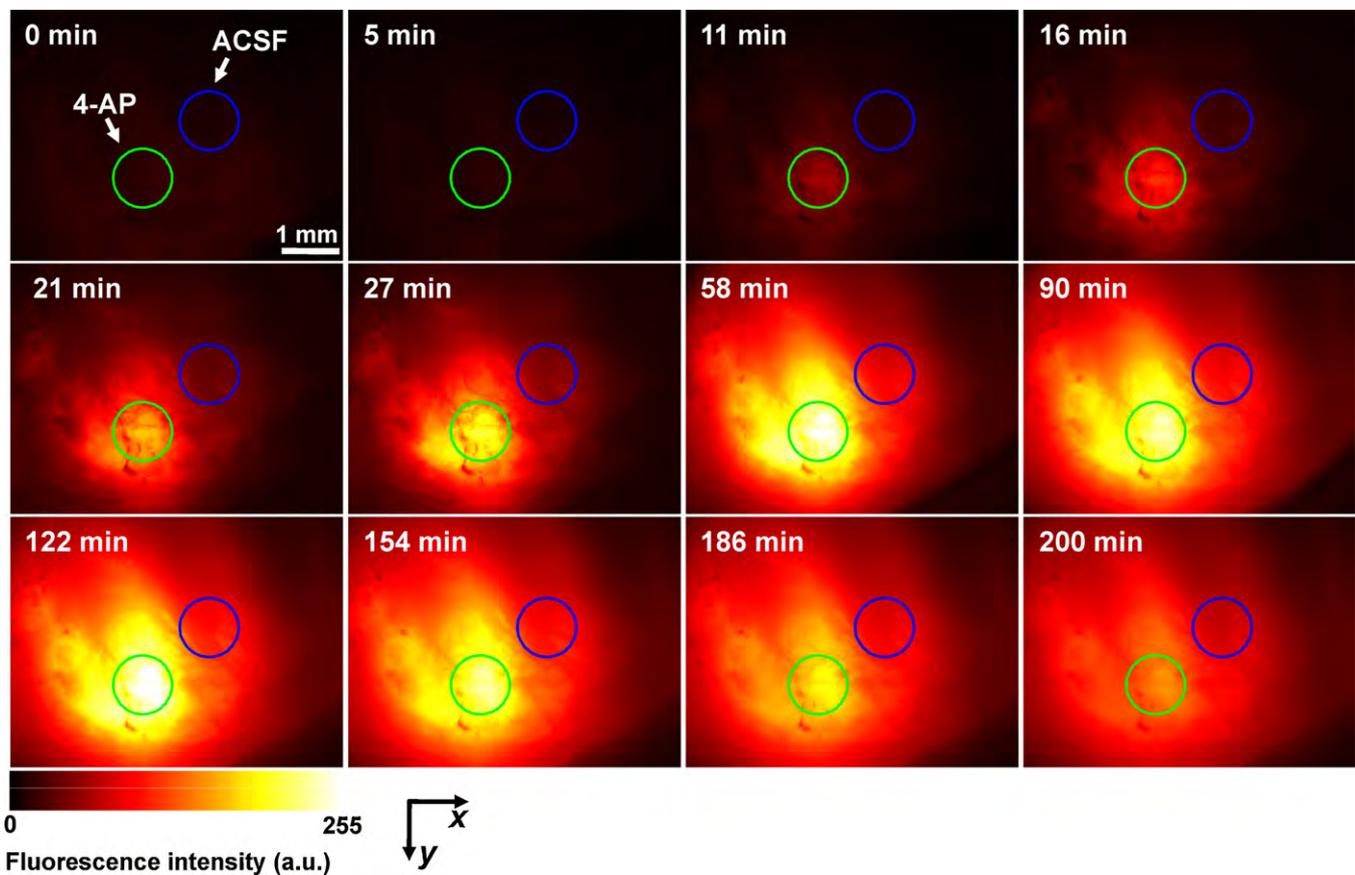
**Fig. 3.** Time course of 2-NBDG accumulation at the injection sites of 4-AP (for epileptic activation, green circles) and ACSF (control, blue circles). (For interpretation of the references to colour in this figure legend, the reader is referred to the web version of this article.)

of 10 s. Images were automatically saved for later analysis. After 10 min, a total of 2 mL of 1% solution of 2-NBDG in Ringer's solution for mammals was continuously injected through the implanted catheter, driven by a syringe pump (Harvard Apparatus). The whole injection took ~15 min at a rate of 0.14 mL/min. Here, a slow, continuous injection was necessary to prolong the circulation time of 2-NBDG and thus help it reach brain cells (Yamada et al., 2009; Sheth et al., 2009).

### 2.6. Image processing

The fluorescence images were analyzed off-line, using an algorithm developed in MATLAB (R2008a, Mathworks). At each time point, the averaged fluorescence intensity of the pixels within 1 mm of the injection sites of 4-AP and ACSF were quantified and normalized to the mean baseline value acquired before the injection of 2-NBDG. The stabilization time, during which the fluorescence intensity reached 90% of the maximum, was calculated for the two injection sites. The quantification results are shown as means with standard deviation, $N = 5$. The statistical test was a paired Student's $t$-test. We considered a $p$-value less than 0.05 to be significant.

### 3. Results

As shown in Figs. 3 and 4A, before the injection of 2-NBDG (0–10 min), fluorescence intensity in the field of view (FOV) was minimal, which indicated relatively little autofluorescence. After the injection of 2-NBDG, the fluorescence intensity in the FOV increased globally. The cortical cells appeared to rapidly take up 2-NBDG and retain it within the cytoplasm. The initial increase

rate around the injection site of 4-AP was significantly greater than that around the injection site of ACSF (Fig. 4B), which reflected a faster uptake of 2-NBDG and thus a greater glucose metabolism. Such hypermetabolism indicated increased neuron activity caused by local epileptic seizures. Moreover, the maximum fluorescence intensity in the area of the epileptic seizures was also higher than that of the control area (Fig. 4A). In our experiments, epileptic foci were clearly marked by such stronger fluorescence signals.

Blood vessels appeared dark in the fluorescence images, because fluorescence emitted by 2-NBDG was mostly absorbed by hemoglobin in red blood cells (Millon et al., 2011; Nitin et al., 2009; Rouach et al., 2008). Because of the lack of 2-NBDG information from blood, the compartment models used for quantifying the glucose metabolic rate in PET studies cannot be directly applied in this study (Dedeurwaerdere et al., 2005; Imamura et al., 2009; Katsuyama et al., 2010).

### 4. Discussion

Potential radiation exposure limits the usage of the radioactive labeled 2-DG analog. In contrast, 2-NBDG solves this issue by providing optical contrast with low toxicity and fast clearance to urine (Millon et al., 2011). Previously it has been demonstrated that the uptake of 2-NBDG correlates well with cellular metabolism in cell studies (Millon et al., 2011; Nitin et al., 2009). *In vitro* studies have also confirmed that epileptic activity increases 2-NBDG traffic in neurons and the glial network (Rouach et al., 2008; Inyushin et al., 2010). Moving one step forward, our *in vivo* results, for the first time, have showed that 2-NBDG is a good indicator of the hypermetabolism caused by epileptic seizures, and may provide a new tool for optically identifying epileptic foci.
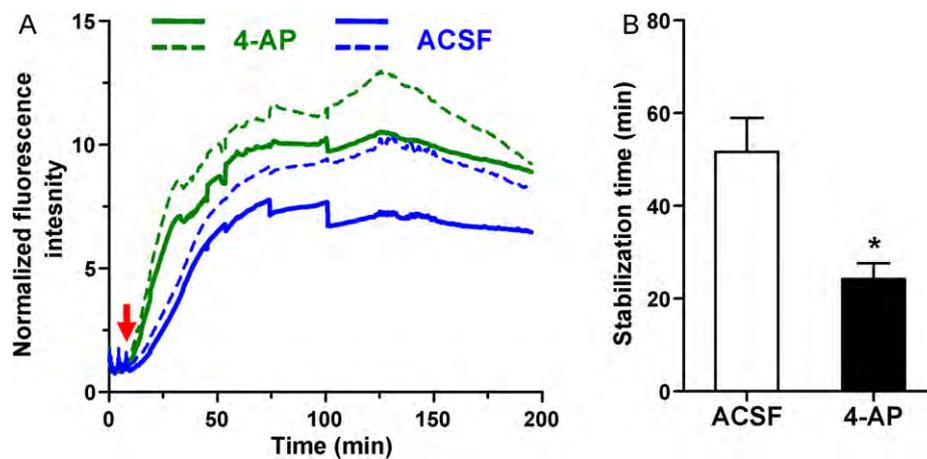
**Fig. 4.** Quantification of 2-NBDG accumulation. (A) The time courses of the normalized fluorescence intensity around the injection sites of 4-AP (for epileptic activation) and ACSF (control), respectively. The red arrow indicates the starting time of 2-NBDG injection via the tail vein. Solid curves indicate the mean value; dashed curves show one standard deviation above the mean. (B) Comparison of the stabilization times (defined as those times reaching 90% of maxima) of 2-NBDG accumulation around the injection sites of 4-AP and ACSF. Statistics: two-tailed paired student's test. *p* value: 0.03. *N* = 5. (For interpretation of the references to colour in this figure legend, the reader is referred to the web version of this article.)

Although current optical methods can be used to localize cortical epileptic foci *in vivo* in an open skull, it is still challenging to apply those methods in subcortical brain structures, especially with an intact skull (Gratton and Fabiani, 2010; Koch et al., 2010). Brain tissue is one of the worst materials for carrying light in the visual or the infrared part of the spectrum (Kim et al., 2010b). Theoretically, it is possible to apply these techniques transcranially, for human subject, especially for the infants, who have more transparent skull and smaller size of the brain, but it needs substantial improvements on the hardware and software as well as the contrast agents. In addition, some modern methods such as diffuse optical tomography (DOT) and photoacoustic tomography (PAT) (Hielscher et al., 2002; Wang et al., 2003; Kim et al., 2010b) may provide new directions. Like FDG used in PET, 2-NBDG has the potential to be used in non-invasive brain imaging in PAT, a newly developed hybrid modality which takes advantage of rich optical contrast and ultrasonic spatial resolution for deep imaging (Mace et al., 2011; Kim et al., 2010b). PAT has highly scalable spatial resolution, imaging speed, and penetration depth, determined by the system configurations (Kim et al., 2010a, b). Using a modified clinical ultrasound array, a penetration depth of ∼5 cm has been demonstrated in biological tissue (Wang et al., 2003). Therefore, by combining 2-NBDG with the excellent imaging capability of PAT, more applications in metabolism-associated studies are expected in the future.

## Acknowledgements

## References

Bahar S, Suh M, Zhao M, Schwartz TH. Intrinsic optical signal imaging of neocortical seizures: the 'epileptic dip'. Neuroreport 2006;17(5):499–503.

Bem M, Badea F, Draghici C, Caproiu MT, Vasilescu M, Voicescu M, et al. Synthesis and properties of some new 4-amino-7 nitrobenzoxadiazole derivatives. ARKIVOC 2007;xiii:87–104.

Bhatia S, Ragheb J, Johnson M, Oh S, Sandberg DI, Lin WC. The role of optical spectroscopy in epilepsy surgery in children. Neurosurg Focus 2008;25(3):E24.

Cang JH, Kalatsky VA, Lowel S, Stryker MP. Optical imaging of the intrinsic signal as a measure of cortical plasticity in the mouse. Vis Neurosci 2005;22(5):685–91.

Dedeurwaerdere S, Cornelissen B, Van Laere K, Vonck K, Achten E, Slegers G, et al. Small animal positron emission tomography during vagus nerve stimulation in rats: a pilot study. Epilepsy Res 2005;67(3):133–41.

Fisher JA, Civillico EF, Contreras D, Yodh AG. In vivo fluorescence microscopy of neuronal activity in three dimensions by use of voltage-sensitive dyes. Opt Lett 2004;29(1):71–3.

Fisher JA, Barchi JR, Welle CG, Kim GH, Kosterin P, Obaid AL, et al. Two-photon excitation of potentiometric probes enables optical recording of action potentials from mammalian nerve terminals in situ. J Neurophysiol 2008;99(3):1545–53.

Gratton G, Fabiani M. Fast optical imaging of human brain function. Front Hum Neurosci 2010;4:52.

Hu S, Maslov K, Tsytsarev V, Wang LV. Functional transcranial brain imaging by optical-resolution photoacoustic microscopy. J Biomed Opt 2009;14(4):040503.

Hielscher AH, Bluestone AY, Abdoulaev GS, Klose AD, Lasker J, Stewart M, et al. Near-infrared diffuse optical tomography. Dis Markers 2002;18(5–6):313–37.

Imamura K, Onoe H, Shimazawa M, Nozaki S, Wada Y, Kato Y, et al. Molecular imaging reveals unique degenerative changes in experimental glaucoma. Neuroreport 2009;20(2):139–44.

Inyushin M, Kucheryavykh LY, Kucheryavykh YV, Nichols CG, Buono RJ, Ferraro TN, et al. Potassium channel activity and glutamate uptake are impaired in astrocytes of seizure-susceptible DBA/2 mice. Epilepsia 2010;51(9):1707–13.

Inyushin MY, Vol'nova AB, Lenkov DN. Use of a simplified method of optical recording to identify foci of maximal neuron activity in the somatosensory cortex of white rats. Neurosci Behav Physiol 2001;31(2):201–5.

Itoh I, Watanabe S, Kirino Y. Mapping of odor-related neuronal activity using a fluorescent derivative of glucose. Neurosci Lett 2006;398(3):224–9.

Itoh Y, Abe T, Takaoka R, Tanahashi N. Fluorometric determination of glucose utilization in neurons in vitro and in vivo. J Cereb Blood Flow Metab 2004;24(9):993–1003.

Kameyama H, Masamoto K, Imaizumi Y, Omura T, Katura T, Maki A, et al. Neurovascular coupling investigated in primary auditory cortex with voltage-sensitive dye imaging and laser-Doppler flowmetry. Brain Res 2008;1244:82–8.

Katsuyama N, Imamura K, Onoe H, Tanaka NK, Onoe K, Tsukada H, et al. Cortical activation during color discrimination task in macaques as revealed by positron emission tomography. Neurosci Lett 2010;484(3):168–73.

Kim C, Erpelding TN, Jankovic L, Pashley MD, Wang LV. Deeply penetrating in vivo photoacoustic imaging using a clinical ultrasound array system. Biomed Opt Express 2010a;1(1):278–84.

Kim C, Favazza C, Wang LH. In vivo photoacoustic tomography of chemicals: high-resolution functional and molecular optical imaging at new depths. Chem Rev 2010b;110(5):2756–82.

Koch SP, Habermehl C, Mehnert J, Schmitz CH, Holtze S, Villringer A, et al. High-resolution optical functional mapping of the human somatosensory cortex. Front Neuroenergetics 2010;14:2–15.

Lee S, Lee M, Koh D, Kim BM, Choi JH. Cerebral hemodynamic responses to seizure in the mouse brain: simultaneous near-infrared spectroscopy–electroencephalography study. J Biomed Opt 2010;15(3):037010.

Ma HT, Zhao MR, Suh M, Schwartz TH. Hemodynamic surrogates for excitatory membrane potential change during interictal epileptiform events in rat neocortex. J Neurophysiol 2009;101(5):2550–62.

Mace E, Montaldo G, Cohen I, Baulac M, Fink M, Tanter M. Functional ultrasound imaging of the brain. Nat Methods 2011;8(8):662–4.

Millon SR, Ostrander JH, Brown JQ, Raheja A, Seewaldt VL, Ramanujam N. Uptake of 2-NBDG as a method to monitor therapy response in breast cancer cell lines. Breast Cancer Res Treat 2011;126(1):55–62.

Nitin N, Carlson AL, Muldoon T, El-Naggar AK, Gillenwater A, Richards-Kortum R. Molecular imaging of glucose uptake in oral neoplasia following topical application of fluorescently labeled deoxy-glucose. Int J Cancer 2009;124(11):2634–42.

Rouach N, Koulakoff A, Abudara V, Willecke K, Giaume G. Astroglial metabolic networks sustain hippocampal synaptic transmission. Science 2008;322(5907):1551–5.

Salek-Haddadi A, Lemieux L, Merschhemke M, Friston KJ, Duncan JS, Fish DR. Functional magnetic resonance imaging of human absence seizures. Ann Neurol 2003;53(5):663–7.

Sheth RA, Josephson L, Mahmood U. Evaluation and clinically relevant applications of a fluorescent imaging analog to fluorodeoxyglucose positron emission tomography. J Biomed Opt 2009;14(6):064014.

Srinivasan VJ, Sakadzic S, Gorczynska I, Ruvinskaya S, Wu WC, Fujimoto JG, et al. Quantitative cerebral blood flow with optical coherence tomography. Opt Express 2010;18(3):2477–94.

Takagaki K, Zhang C, Wu JY, Ohl FW. Flow detection of propagating waves with temporospatial correlation of activity. J Neurosci Methods 2011;200(2):207–18.

Tsytsarev V, Fukuyama H, Pope D, Pumbo E, Kimura M. Optical imaging of interaural time difference representation in rat auditory cortex. Front Neuroeng 2006;2:2.

Tsytsarev V, Hu S, Yao J, Maslov K, Barbour DL, Wang LW. Photoacoustic microscopy of microvascular responses to cortical electrical stimulation. J Biomed Opt 2011;16(7):076002.

Tsytsarev V, Pope D, Pumbo E, Yablonskii A, Hofmann M. Study of the cortical representation of whisker directional deflection using voltage-sensitive dye optical imaging. Neuroimage 2010;53(1):233–8.

Tsytsarev V, Premachandra K, Takeshita D, Bahar S. Imaging cortical electrical stimulation in vivo: fast intrinsic optical signal versus voltage-sensitive dyes. Opt Lett 2008;33(9):1032–4.

Yamada A, Momosaki S, Hosoi R, Abe K, Yamaguchi M, Inoue O. Glucose utilization in the brain during acute seizure is a useful biomarker for the evaluation of anticonvulsants: effect of methyl ethyl ketone in lithium-pilocarpine status epilepticus rats. Nucl Med Biol 2009;36(8):949–54.

Yang XF, Duffy DW, Morley RE, Rothman SM. Neocortical seizure termination by focal cooling: temperature dependence and automated seizure detection. Epilepsia 2002;43(3):240–5.

Wang X, Pang Y, Ku G, Xie X, Stoica G, Wang LV. Noninvasive laser-induced photoacoustic tomography for structural and functional in vivo imaging of the brain. Nat Biotechnol 2003;21(7):803–6.